Numerical study of guided modes in arrays of metallic nanowires

C. G. Poulton,* M. A. Schmidt, G. J. Pearce, G. Kakarantzas, and P. St.J. Russell

Max-Planck Research Group (IOIP), University of Erlangen-Nuremberg, Günther-Scharowsky-Str. 1/Bau 24, 91058 Erlangen, Germany

**Corresponding author: cpoulton@optik.uni-erlangen.de*

Received February 6, 2007; revised March 27, 2007; accepted April 1, 2007; posted April 12, 2007 (Doc. ID 79833); published June 5, 2007

We numerically investigate the band structure and guided modes within arrays of metallic nanowires. We show that bandgaps appear for a range of array geometries and that these can be used to guide light in these structures. Values of attenuation as low as 1.7 dB/cm are predicted for arrays of silver wires at communications wavelengths. This is more than 100 times smaller than the attenuation of the surface plasmon polariton modes on a single silver nanowire. © 2007 Optical Society of America

OCIS codes: 060.2310, 240.6680.

In their most common form, photonic crystal fibers (PCFs) guide light by means of an array of air channels in a silica matrix [1]. The high refractive index contrast between silica and air permits the formation of photonic bandgaps (PBGs) that can be used to trap light inside a hollow core. We consider here the guidance properties of PCF in which the air channels are replaced with metallic nanowires. In such structures the very high permittivity contrast is likely to increase the robustness of guided modes to bends and other structural deformations, and field enhancements at the metal–glass interfaces could be used to increase nonlinear interactions. In addition it has recently been demonstrated [2] that the guided light can interact strongly with the surface plasmon polariton (SPP) modes in the wires, and it has been suggested that this can be used for sensors and fiber-integrated optoelectronic components [2,3]. Here we calculate the positions of the PBGs for a triangular lattice of nanowires and calculate the effective index and attenuation of the fundamental guided mode resulting from removal of a single wire.

A necessary condition for achieving guidance is the existence of a PBG below the light line of the host material surrounding the wires. For this reason we first consider the calculation of the band structure of the cladding, which we consider to be a triangular lattice of silver nanowires (pitch Λ, diameter d) embedded in a matrix of fused silica. The permittivity of the metal is assumed to be accurately described by the Drude model [4]:

$$\epsilon_m = \epsilon_\infty - \frac{\omega_p^2}{\omega^2 + i\omega\omega_\tau}, \tag{1}$$

where $\omega = 2\pi f$ is the angular frequency, ω_p and ω_τ are the plasma frequency and damping frequency, respectively, and ϵ_∞ is the permittivity in the high-frequency limit. In the following calculations we have used the parameters

$$\omega_p = 2\pi \times 2175 \text{ THz}, \ \omega_\tau = 2\pi \times 4.35 \text{ THz},$$

and $\epsilon_\infty = 1$, which have been shown to give very good agreement with measured values over a wide frequency range [5]. The dispersion of the silica matrix was modeled using Sellmeier equations [6].

Because the frequency dependence of the material properties breaks the scale invariance of Maxwell's equations, it is necessary to consider a fixed operating frequency and then calculate the band structure for a range of geometries having the appropriate values of ϵ_m and ϵ_s. We therefore choose the frequency

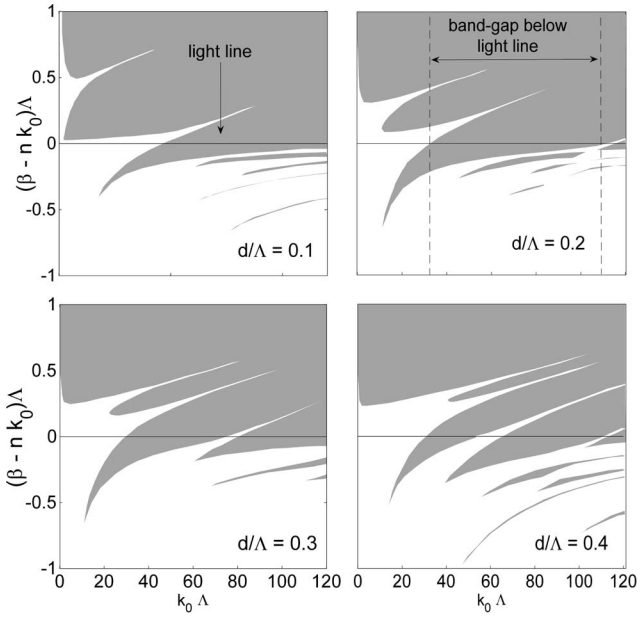

Fig. 1. Presence of bandgaps (gray) as a function of normalized frequency $k_0\Lambda$ in a silica matrix of refractive index n, for different wire diameters d. All calculations were performed for the optical properties of silver and silica at $\lambda_0 = 1.55$ μm, neglecting material loss. The plasmon modes appear as resonances above the light line. Because of the strong interaction between the plasmon modes, large normalized frequencies ($k_0\Lambda > 30$) are necessary to establish a gap below the light line.

0146-9592/07/121647-3/$15.00

$f=193.4$ THz, corresponding to a vacuum wavelength $\lambda_0=1.55$ μm, at which the permittivities ϵ_m of the metal and ϵ_s of silica are $\epsilon_m=-125.3+2.843i$ and $\epsilon_s=2.085$, relative to the permittivity of free space. For these and subsequent bandgap calculations, we model a structure in the absence of material absorption in the metal ($\mathrm{Im}[\epsilon_m]=0$). This has the advantages of indicating where the bandgaps would occur in a loss-free structure and of highlighting the effects of optical absorption once it is introduced. Removing absorption also means that both the frequency and the Bloch wave vector remain real valued in the calculations, avoiding the difficult business of distinguishing between evanescent decay (caused by bandgaps or leakage) and decay caused by material absorption. For all calculations we used the multipole method [7], which is the fastest and most accurate algorithm for arrays of high-contrast circular inclusions.

The location of the bandgaps is plotted in Fig. 1 for a number of different wire diameters, in terms of normalized frequency $k_0\Lambda=\omega\Lambda/c$ and mode propagation constant β. The plasmon modes are clearly visible as resonances, or photonic band windows [8], above the light line. The existence of a PBG that can be used to guide a defect mode depends on the positions of the cutoffs of these plasmon modes as well as on the breadth of the resonances as they cross the light line. The spectral broadening is caused by coupling between the modes of individual inclusions, and in the vicinity of cutoff this can be shown [9] to increase rapidly as the mode order decreases. In contrast to the situation for silica–air PCF, the significant broadening of the first two SPP modes above the light line precludes gap formation, and so large values of $k_0\Lambda$ (>30) are necessary to achieve a PBG for all values of d/Λ between 0.05 and 0.55. For the material properties given above, this choice of $k_0\Lambda$ corresponds to a pitch of at least 8 μm.

We now consider the case of a finite guiding structure and include the material absorption of the metal nanowires. To achieve a PBG at $\lambda_0=1.55$ μm, we choose a structure with a pitch of $\Lambda=10$ μm and wire diameter $d=1.5$ μm. For this fixed value of pitch we are now free to include the material dispersion of the metal wires and of the silica matrix in both mode and bandgap calculations. We consider the simplest case, that of a defect PCF waveguide consisting of three rings of wires with a single wire removed from the center of the array to form the guiding core. For this finite structure the multipole method can be used to calculate the effective refractive index of the fundamental guided mode, the imaginary part of which gives the attenuation.

The effective refractive index $n_{\mathrm{eff}}=\beta/k_0$ of the fundamental guided mode is shown in Fig. 2(a). For this structure the positions of the frequency-dependent bandgaps have also been calculated. The fundamental mode can be seen to exist within the gap below the light line and undergoes an anticrossing with the second order ($m=2$) plasmon mode at a frequency of $f=253$ THz. The attenuation of the fundamental mode is shown in Fig. 2(b) and is compared with the attenuation of the SPP modes for a single wire with

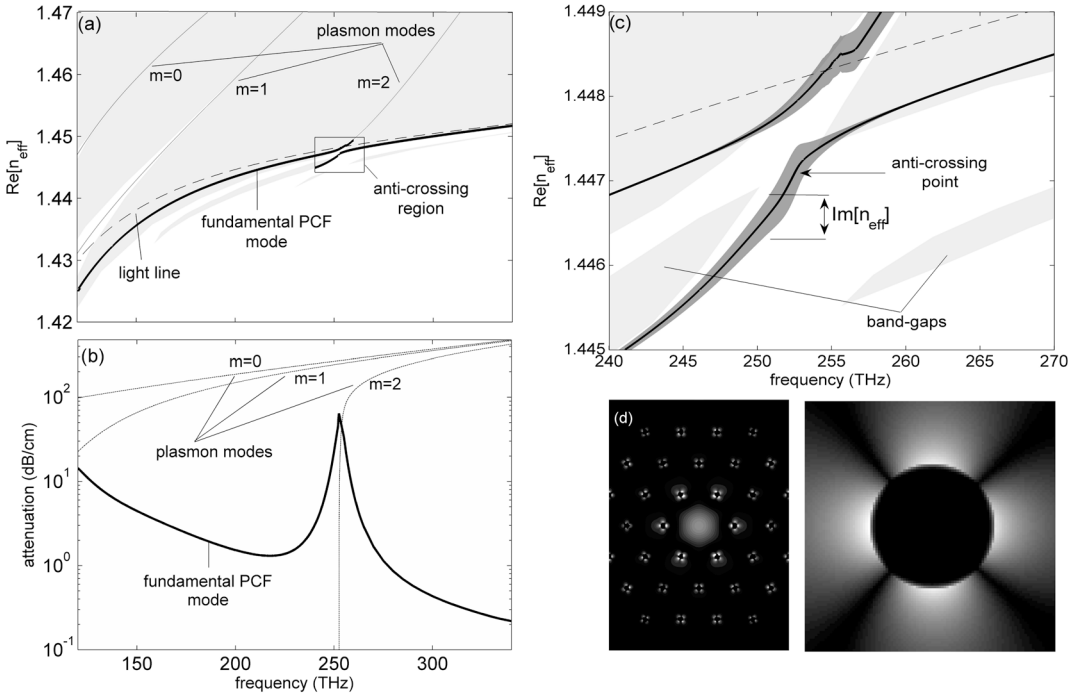

Fig. 2. (a) Fundamental guided mode and bandgaps (gray regions) of an array of nanowires consisting of silver cylinders in a silica matrix, with $d=1.5$ μm and $\Lambda=10$ μm. (b) Attenuation in the fundamental guided mode (solid), as compared with the first three plasmon modes of a single wire (dotted). (c) Magnified view of the anticrossing point. The imaginary part of the effective index ($\mathrm{Im}[n_{\mathrm{eff}}]$) is depicted as the shaded region on either side of the mode itself and shows the relative magnitude of the attenuation. (d) Real part of the Poynting vector of the guided mode at the anticrossing point, on the lower branch ($f=253$ THz, $\lambda_0=1.18$ μm). The closeup shows that the fields have a strongly quadrupolar dependence.

the same physical properties as the components of the array. We can see that the attenuation for this guided mode is more than 100 times smaller than that of the plasmon modes above the light line; this is because most of the light of the guided mode is confined to the nonlossy core region. For the mode at $\lambda_0 = 1.55\ \mu$m the attenuation has been calculated to be 1.7 dB/cm, which is relatively small when compared with other metallic waveguides at communications frequencies [5].

We see in Fig. 2(c) that the anticrossing between the fundamental guided mode and the second-order SPP mode is accompanied by a substantial increase in attenuation as the mode traverses the resonances between the bandgaps. Within this region we see [Fig. 2(d)] that the mode extends strongly into the array, and one can also observe a strong quadrupolar component in the field distribution around the cylinders. On one side of the anticrossing the fundamental mode undergoes a smooth transition to an array of surface-plasmon resonances, while on the other side the fundamental mode becomes a sum of Bloch modes with appropriate symmetry.

In silica–air PCF the attenuation can be reduced by adding additional rings of wires around the core, thereby increasing the distance over which the light must tunnel through the PBG to escape. This is not necessarily the case with the metallic PCF studied here, where ohmic losses will play an important role in the attenuation. To examine the relative strengths of leakage and material loss, we have calculated the separate contribution from these loss mechanisms for structures having one-, two-, and three-ring layers of wires surrounding the guiding core (Fig. 3). The ohmic loss of the mode was calculated by using an overlap integral between the modal fields and the material loss of the metal [10]. The leakage loss was calculated by integrating the outgoing energy per unit of length over a perimeter external to the waveguide. This quantity can also be calculated by arbitrarily setting the imaginary part of ϵ_m to zero and computing the overall loss in this artificial case—this method was also used and provided us with an additional check on the validity of our numerical simulations. As can be seen in Fig. 3, the leakage loss indeed decreases rapidly with additional layers of wires. We observe, however, that the material loss dominates over a broad range of frequencies. In the vicinity of the resonance both loss mechanisms become important, because of stronger coupling with the SPP modes, which causes both a larger material loss and increased transport of light into the region outside the core. We observe that optimal light confinement can be achieved with as few as two surrounding rings.

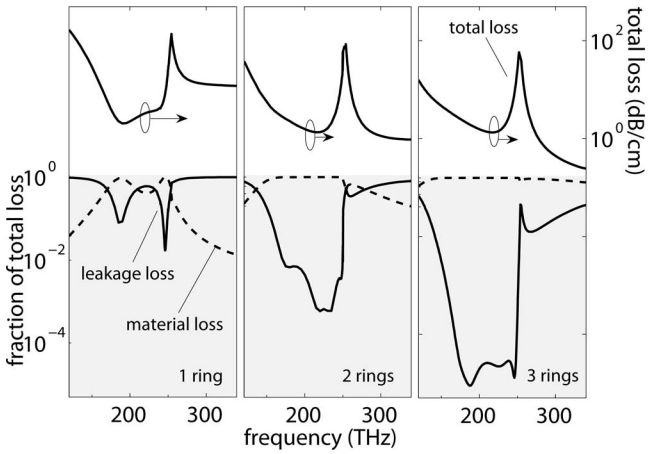

Fig. 3. Total attenuation (top) and comparison of leakage and material loss (bottom) of the fundamental mode in structures possessing one, two, and three rings of wires surrounding the core. The leakage loss decreases rapidly with each successive layer, and the resulting total attenuation is dominated by the material loss.

References

1. P. St.J. Russell, J. Lightwave Technol. **24**, 4729 (2006).
2. B. T. Kuhlmey, K. Pathmanandavel, and R. C. McPhedran, Opt. Express **14**, 10851 (2006).
3. P. J. A. Sazio, A. Amezcua-Correa, C. E. Finlayson, J. R. Hayes, T. J. Scheidemantel, N. F. Baril, B. R. Jackson, D.-J. Won, F. Zhang, E. R. Margine, V. Gopalan, V. H. Crespi, and J. V. Badding, Science **311**, 1583 (2006).
4. M. A. Ordal, L. L. Long, R. J. Bell, S. E. Bell, R. R. Bell, R. W. Alexander, and C. A. Ward, Appl. Opt. **22**, 1099 (1983).
5. I. El-Kady, M. M. Sigalas, R. Biswas, K. M. Ho, and C. M. Soukoulis, Phys. Rev. B **62**, 15299 (2000).
6. G. P. Agrawal, *Nonlinear Fiber Optics* (Academic, 2001).
7. T. P. White, B. T. Kuhlmey, R. C. McPhedran, D. Maystre, G. Renversez, C. M. de Sterke, and L. C. Botten, J. Opt. Soc. Am. B **19**, 2322 (2002).
8. P. St.J. Russell, T. Birks, and F. D. Lloyd-Lucas, *Photonic Bloch Waves and Photonic Band Gaps* (Plenum, 1995), p. 607.
9. T. A. Birks, G. J. Pearce, and D. M. Bird, Opt. Express **14**, 9483 (2006).
10. A. Yariv and P. Yeh, *Optical Waves in Crystals* (Wiley, 1984), pp. 473–477.